

## Interference in interacting quantum dots with spin

Daniel Boese\*

*Institut für Theoretische Festkörperphysik, Universität Karlsruhe, D-76128 Karlsruhe, Germany*Walter Hofstetter<sup>†</sup>*Theoretische Physik III, Elektronische Korrelationen und Magnetismus, Universität Augsburg, D-86135 Augsburg, Germany*

Herbert Schoeller

*Institut für Theoretische Physik A, RWTH Aachen, D-52056 Aachen, Germany*

(Received 25 January 2002; revised manuscript received 17 June 2002; published 27 September 2002)

We study spectral and transport properties of interacting quantum dots with spin. Two particular model systems are investigated: lateral multilevel and two parallel quantum dots. In both cases different paths through the system can give rise to interference. We demonstrate that this strengthens the multilevel Kondo effect for which a simple two-stage mechanism is proposed. In parallel dots we show under which conditions the peak of an interference-induced orbital Kondo effect can be split.

DOI: 10.1103/PhysRevB.66.125315

PACS number(s): 73.63.Kv, 71.27.+a, 72.15.Qm, 73.23.Hk

### I. INTRODUCTION

Interference is one of the key phenomena of quantum physics. The prototype experiment is the famous double slit experiment where interference between two possible paths leads to an oscillatory pattern on the detection screen. In those experiments the phase difference is of geometrical nature, i.e., one of the paths is longer. A phase difference can also be introduced due to an enclosed magnetic flux. In mesoscopic physics such an experiment is referred to as the Aharonov-Bohm (AB) ring, where the current through the AB ring shows oscillations as a function of the magnetic field threading the ring.

An AB ring can be used as an interferometer, where the object under consideration is placed in one of the ring's arms, and the phase is tuned by changing the object's parameters. In this way, one can measure the transmission phase of an interacting system, like a quantum dot (QD),<sup>1-8</sup> which in general (and especially when tuned to the Kondo regime) has a complicated many-body ground state. In recent experiments quantum dots have been put into both arms,<sup>5</sup> in some cases so close that a strong capacitive Coulomb interaction between the two dots has been introduced (see Fig. 1, upper right, for an illustration). The two paths are no longer independent, but influence each other considerably. In a naive classical picture one could imagine that interaction would destroy interference, as making use of one path effectively closes the other. To answer this question the phase dependence of the current needs to be studied, and it turns out that the current indeed can be modulated. Note that such systems are of fundamental interest also because they can be viewed as artificial molecules where, e.g., entangled states can be observed in transport and noise.<sup>9</sup>

The coherence of quantum-mechanical states has recently become a topic of broad interest, as it is fundamental to applications such as quantum computing and to many phenomena such as the Kondo effect. In AB interferometers coherence is essential for interference to take place. Therefore they constitute good test grounds to study the gain and loss

of coherence in nanoscale devices, as was demonstrated by Buks and co-workers<sup>10</sup> who demonstrated controlled dephasing by intentionally introducing decoherence in one of the arms.

Single quantum dots can constitute interacting interferometers by themselves, since they have in general many levels that can participate in transport. In contrast to vertical QDs, the states in lateral QDs are labeled by a nonconserved quantum number. Furthermore, a multilevel structure is also relevant to other systems, such as single atom contacts,<sup>11</sup> heavy fermion compounds (e.g., studied by photoemission<sup>12</sup>), or general molecular electronics setup, where many channels can interfere. The capacitive Coulomb interaction between two dots is replaced by the onsite interaction between different levels. The tunability of the phase with magnetic fields, however, is lost, although some tunability using gates is still present. Nevertheless, it is instructive to study interference

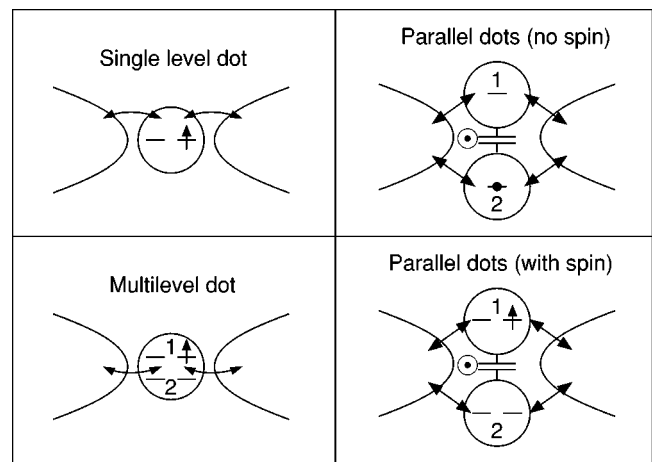


FIG. 1. The four quantum dot setups of relevance to this work. A dot with one single, spin-degenerate level (top left); two parallel dots with one spinless level each, enclosing a flux (top right); a dot with two levels and spin (bottom left); and two parallel dots with one level with spin (bottom right). The paper is mainly concerned with the physics of the systems displayed in the bottom panels.

effects in single quantum dots, since in general many dot levels participate in the transport, see Fig. 1, bottom left. A prominent example is the occurrence of the Fano effect<sup>13–15</sup> with its characteristic line shape, which is due to interference between a resonant and a nonresonant transport channel. Moreover, it is often assumed that one level dominates the transport, while the others are only very weakly coupled. We show that such a situation, even if not present initially, can be created dynamically.

In most quantum dots the levels are spin degenerate in the absence of a magnetic field. The effect of this degeneracy is manifold. As electrons with different spin cannot interfere with each other their role is contrary to interference. The difference is indeed drastic, as on one side parallel QDs can be opaque due to destructive interference, while on the other hand the spin in a single QD can form a Kondo ground state leading to perfect transparency.<sup>3,16,17</sup> Accounting for the spin degree of freedom is therefore a necessary step towards more realistic models of QDs.

In the course of this work we will show that the combination of interference and Kondo physics in multilevel QDs leads to a stronger Kondo effect. However, this effect is caused by a new, effective level and thus resembles single level Kondo physics.

Interference can be described by a tunneling Hamiltonian with at least one nonconserved index. Therefore the tunneling part has the general form  $H_T = \sum_{kr\sigma l n} T_{ln}^{kr} a_{kr\sigma}^\dagger c_{\sigma n l} + \text{H.c.}$  The reservoir operators are denoted by  $a_{kr\sigma n}$ , the dot operators by  $c_{\sigma n l}$ . The quantum number  $l$  is present only in the QD Hamiltonian, it is the analog of the paths. The index must not be conserved in tunneling, as otherwise the electrons would not know of each other (as if they would be in different reservoirs), ruling out any interference.  $k$  denotes the wave vectors and  $n$  an additional conserved quantum number in reservoir  $r$ . The conserved index  $n$  can be due to symmetries present in the leads and dot, such as a rotational symmetry in some vertical quantum dots giving rise to an angular momentum quantum number. As seen from the structure of the tunneling Hamiltonian, they play a similar role as the spin and can cause and increase a Kondo effect (orbital Kondo effect).<sup>18–21</sup> In lateral quantum dots such symmetries are typically not present and we suppress those indices from now on.

Interference is also interesting from a technical and fundamental point of view. The nonconservation of quantum numbers leads to nonvanishing off-diagonal elements of the reduced density matrix of the local system, which describe the coherence of states. Their presence explains why transport in first order, which usually is referred to as sequential tunneling, can still be coherent.<sup>22</sup> Moreover, nonequilibrium one-particle Green's functions are needed, even to describe the linear response regime.

The coupling to the leads can be so strong that perturbation theory may not be sufficient anymore. For the Anderson model this is referred to as the regime where Kondo correlations develop. Also for a simple model of two spinless dot levels it has been shown that near destructive interference the model can be mapped onto an effective Kondo model showing strong-coupling behavior in a peculiar way. A phase tran-

sition of the type Ruderman-Kittel-Kasuya-Yosida vs Kondo tunable by a magnetic flux has been predicted.<sup>23,24</sup>

Our theoretical results in this work were mainly obtained by using Wilson's numerical renormalization group,<sup>25–27</sup> supplemented by additional scaling calculations. In the following section we introduce and discuss the model. In a qualitative discussion we summarize the conclusions drawn from a spinless model and generalize them to the present case. We then focus on the Kondo effect multilevel QDs in Sec. IV and on the interference-induced orbital Kondo effect in parallel QDs in Sec. V.

## II. MODEL

We introduce the following model Hamiltonian of two parallel, interacting QDs connected to two electron reservoirs  $r \in \{R, L\}$  via tunnel barriers, see also Fig. 1, bottom right. Each quantum dot (labeled  $l \in \{1, 2\}$ ) is modeled by an Anderson-type Hamiltonian of a single spin-degenerate level,

$$H = \sum_{kr\sigma} \epsilon_{kr} a_{kr\sigma}^\dagger a_{kr\sigma} + \sum_{l\sigma} \epsilon_l c_{l\sigma}^\dagger c_{l\sigma} + \sum_{(l\sigma) \neq (l'\sigma')} U_{ll'} n_{l\sigma} n_{l'\sigma'} + \sum_{krl\sigma} (T_l^r a_{kr\sigma}^\dagger c_{l\sigma} + \text{H.c.}). \quad (1)$$

The third term represents the Coulomb interaction, where  $U_{ll}$  is of the order of the intradot charging energy (in dot  $l$ ), and  $U_{12}$  reflects the interdot charging energy. To minimize the number of parameters involved we take  $U_{ll'} = U$ , as they are similar in order of magnitude.<sup>5</sup> We are interested in the case of strong interactions, i.e., when  $U$  is the largest energy of the system, requiring an explicit treatment. This allows to restrict the discussion to two charge states, i.e., number of electrons in the dot  $N \in \{0, 1\}$ , and hence exchange terms may be neglected. This is not the case for  $N > 1$ , where interesting physics can be observed.<sup>28</sup> The tunneling matrix elements  $T_l^r$  are assumed to be independent of spin and wave vector. If a magnetic flux is enclosed one can either distribute the accumulated phase equally on the four  $T_l^r$ , or equivalently attach the phase  $\phi$  to a single element. We choose the latter, i.e., we take  $T_2^L(\phi) = T_2^L \exp(i\phi)$ , and furthermore assume the matrix elements to be real and symmetric with respect to left and right (i.e.,  $T_l^L = T_l^R = T_l$ ). Together with the density of states in the leads  $\rho_0$  (which is assumed to be independent of energy) we introduce the coupling constants  $\Gamma_{ll'} = 2\pi\rho_0 \sum_{i=r, l} T_l^i T_{l'}^{i,*}$ . The magnetic field shall be small enough such that only the AB phase is influenced and Zeeman and orbital shifts can be neglected.

We introduce another set of dot states that simplifies the discussion later on (see Fig. 2 for an illustration of the physical meaning of these states). With  $T_{1/2}$  being real (the  $\phi$  dependence we take explicitly) and  $\tau = \sqrt{T_1^2 + T_2^2}$  we can write

$$f_{1/2\sigma} = \frac{T_{1/2} c_{1\sigma} \pm T_{2/1} c_{2\sigma}}{\tau}. \quad (2)$$

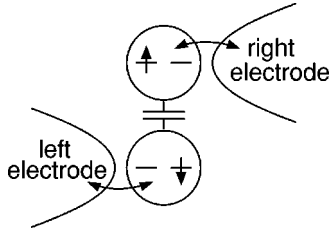


FIG. 2. Destructive interference leads to a Kondo-like situation. A geometric (left/right) pseudospin is introduced. The quantum dots interact capacitively.

Together with the definition  $\epsilon_{1/2} = \epsilon \pm \delta\epsilon/2$  this yields the new Hamiltonian

$$\begin{aligned}
 H = & \sum_{\sigma} \epsilon (n_{f_{1\sigma}} + n_{f_{2\sigma}}) - \frac{\delta\epsilon T_1 T_2}{\tau^2} (f_{1\sigma}^{\dagger} f_{2\sigma} + f_{2\sigma}^{\dagger} f_{1\sigma}) \\
 & + U \sum_{(f_i\sigma) \neq (f_j\sigma')} n_{f_i\sigma} n_{f_j\sigma'} + \sum_{k\sigma} \left[ \tau a_{kR\sigma}^{\dagger} f_{1\sigma} \right. \\
 & \left. + a_{kL\sigma}^{\dagger} \left( \frac{T_1^2 + T_2^2 e^{i\phi}}{\tau} f_{1\sigma} + \frac{T_1 T_2}{\tau} (1 - e^{i\phi}) f_{2\sigma} \right) + \text{H.c.} \right] \\
 & + \sum_{kr\sigma} \epsilon_{kr} a_{kr\sigma}^{\dagger} a_{kr\sigma}. \quad (3)
 \end{aligned}$$

It is obvious that for  $\delta\epsilon=0$  the cases  $\phi=0$  and  $\phi=\pi$  plus  $T_1=T_2$  are special and should be considered separately. Note that it is the density of states (DOS) of the  $f_{1\sigma}$  level that is relevant for the transport. This becomes clear when considering the current from the right reservoir into the dot (which due to charge conservation equals the total current). As only the  $f_{1\sigma}$  level couples to the right reservoir it must be the DOS of this level that determines the current. In the following we assume that the couplings  $\Gamma_{ll'} = \Gamma$  are independent of the level indices.

It is useful to compare the above Hamiltonian Eq. (1) to that of a single, lateral, multilevel QD (see Fig. 1, bottom left). In this case the index  $l$  labels the dot states and the sum runs in general over many such states. Yet, for large level spacing one may approximate the situation by taking only two states. A generalization to many levels will be given in Sec. IV. The interaction parameters  $U_{ll'}$  now corresponds to intradot interactions. Taking them all equal is a standard assumption (constant interaction model). Thus we see that, apart from the AB tunability, Eq. (1) also describes multilevel, single QDs.

We note that this model goes beyond previous work. Inoshita *et al.*<sup>29</sup> have considered only the case of vanishing AB phase, while the Coulomb interaction was treated approximately. In Ref. 30, König and co-workers neglected interactions, phase dependencies, and spin. In a more recent work those were mostly accounted for, their focus, however, was on the role of phase coherence in independent (i.e., non-interacting) arms of the AB ring.<sup>22,31</sup> Silvestrov and Imry<sup>32,33</sup> investigated a multilevel QD model (i.e., no phase dependence), but concentrated on the limit of one broad and one

narrow level, utilizing perturbative arguments. Their model of strongly and weakly coupled levels is related to the Fano effect studied in Refs. 14 and 15 and measured by Göres and co-workers.<sup>13</sup> In a previous work of us,<sup>23</sup> a more simple model, which neglects the spin, was addressed. Models with spin but no dot-dot interaction have been studied in Refs. 34 and 9, while in Ref. 35, which incorporates interaction, only special AB phases have been investigated, and Ref. 36 is concerned with occupation numbers of the ground state.

### III. QUALITATIVE DISCUSSION OF GENERAL PROPERTIES

We start with a discussion of multilevel dots with no phase, i.e.,  $\phi=0$ . It is well known that QDs with a single level (the two-lead Anderson model) display Kondo physics for temperatures below the Kondo scale

$$T_K \sim \frac{\sqrt{U\Gamma}}{2} \exp\left(\frac{\pi\epsilon(\epsilon+U)}{\Gamma U}\right). \quad (4)$$

The manifestation of this is an increased density of states at the Fermi edge resulting in an increased conductance of the dot, which for  $T \rightarrow 0$  even may reach the unitary value of  $2e^2/h$ . It is *a priori* not clear if and how this prevails when more orbitals participate.

The physics of two and more orbitals without spin has been addressed before, and it was found that instead of Kondo physics a hybridization

$$\Delta \sim \frac{\Gamma}{2\pi} \ln \frac{E_C}{\omega_c} \quad (5)$$

of the two levels is introduced.<sup>23,24</sup> Here  $E_C$  is of the order of the charging energy and  $\omega_c$  represents the lower cutoff, which is determined by, e.g.,  $\Gamma$  or  $T$ . This scale  $\Delta$  is much larger than the exponentially small Kondo scale, and it leads to a shoulder in the DOS of order  $\Delta$  above the Fermi edge. The weight of this shoulder is related to the level splitting and vanishes for  $\delta\epsilon \rightarrow 0$  and its width is roughly half the width of the main excitation, i.e.,  $\Gamma/2$ .

In order to understand what happens for two orbitals with spin we perform a Schrieffer-Wolff transformation (see Appendix for details), followed by a poor man's scaling approach. In this transformation the hybridization is created and thus the level splitting increases until it becomes of the same order as the flow parameter  $\omega_c$ . Then the upper  $f_{2\sigma}$  level is too high in energy, decouples, and thus does not participate anymore. The scaling proceeds with the renormalized single  $f_{1\sigma}$  level. Hence we have found a two-stage situation. First one level is pushed upwards until it is out of reach, then in the second step the remaining, renormalized level makes the Kondo effect alone.

The picture is slightly different for the parallel QDs. The flux enclosed leads to destructive interference and the current can even go to zero. The energy scale  $\Delta$  is modified by a factor  $(1 + \exp[i\phi])/2$  and thus vanishes for  $\phi=\pi$ . In this case the model can be mapped onto an effective Kondo

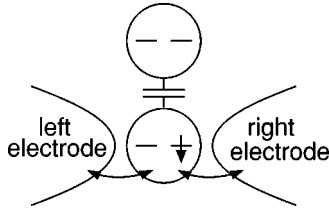


FIG. 3. For vanishing level spacing and phase, the QD can be mapped onto a QD model as shown. Only one QD (the  $f_{1\sigma}$  level) is coupled to the leads. The other one (the  $f_{2\sigma}$  level) influences the transport only by electrostatic means. For strong interactions the upper dot acts like a switch: When it is occupied the current is blocked, when it is empty, the lower dot behaves like a single dot. An exact solution of this model can be found in Ref. 24.

model. When the spin is included this is still the case and a more strong Kondo effect takes place as will be discussed in Sec. V A.

#### IV. MULTILEVEL QUANTUM DOTS

In this section we focus on the interesting regime of levels below the Fermi edge and at low temperatures. This is the regime of the Kondo effect, where correlation effects dominate and the dot's spin is screened by the electrons in the leads. For clarity we mention again that  $\phi=0$  in this section.

In a first step we look at the case of two degenerate levels in the dot. In Fig. 3 we show results for the total spectral density. There are four possible states an electron can occupy in the dot, characterized by a spin index, which is conserved in tunneling, and an orbital index, which is not conserved. As discussed before, this is equivalent to one strongly coupled level and one decoupled one. Hence we see single-level Kondo physics with greatly increased  $T_K$ . The big increase of  $T_K$  compared to the factor of  $\sqrt{2}$  in the tunneling matrix element can be easily understood from the definition of  $T_K$  which involves the coupling  $\Gamma$  exponentially.

In the second step we allow the two orbitals to be different in energy. One might speculate that this should lead to the appearance of side or satellite Kondo peaks. However, in Fig. 4 we demonstrate that single-level Kondo physics is effectively seen for split levels as well. With increasing splitting the Kondo peak becomes narrower, signaling a decreasing  $T_K$ . At the same time the shoulder discussed in the previous section becomes visible and progressively moves to higher frequencies. This can be understood from the Schrieffer-Wolff transformed Hamiltonian in the  $f$ -basis (see Appendix for details). Equation (A6) shows that only the  $f_{1\sigma}$  level generates the Kondo resonance.

In the scaling language it can be thought of as a two-step process. First the tunnel-splitting is generated by integrating out high-energy modes, while the scaling cut-off  $\omega$  is reduced from a value of the order of the interaction strength  $U$  (nothing important happens between  $U$  and the band cutoff  $D$ , if  $D$  is larger) downwards. When integrating out terms like  $a_{k\sigma}^\dagger a_{k'\sigma} c_{1\sigma}^\dagger c_{2\sigma}$ , only the hybridization term  $c_{1\sigma}^\dagger c_{2\sigma}$  remains with a strength  $\Delta$  as described before. The creation of the hybridization stops when the scaling parameter  $\omega$  reaches an intermediate energy scale  $\omega_c$ , where  $\omega_c$  and one of  $\Delta$ ,  $\Gamma$ ,

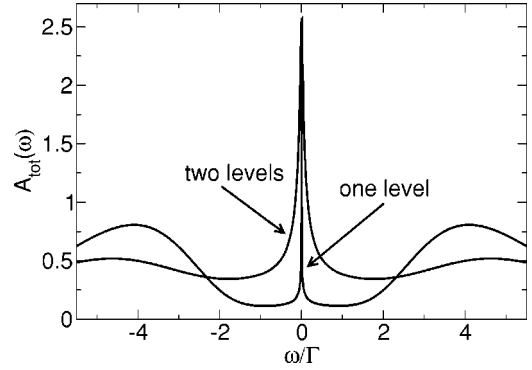


FIG. 4. Effective density of states for the Kondo effect with one and two orbitals. The Kondo temperature increases strongly with the number of levels. Parameters for the symmetric dot are in units of  $\Gamma$ :  $2\pi U=50$ ,  $\epsilon_1=\epsilon_2=-25/2\pi$ ,  $2\pi D=25$ ,  $\phi=0$ ,  $T=0$ .

or  $T$  are of similar order. Scaling breaks down at that point, and we first need to diagonalize the dot states. Then, however, one level is pushed up, above  $\omega_c$ , and it can no longer contribute to scaling, while the other one—the broad  $f_{1\sigma}$  level—stays in the window. The scaling now continues and gives the usual Kondo physics of a single, but modified level. It should be noted that this reflects the strong coupling behavior of the problem, i.e., all energy scales are important and contribute equally. This is in contrast to the flow of the hybridization which stops at an intermediate energy scale and is separated from the problem before the strong coupling behavior is reached. In the inset of Fig. 4 we show the partial spectral densities of the upper and lower level which demonstrate that the lower level. (For this level splitting the lower and the  $f_{1\sigma}$  level have significant overlap) alone produces the Kondo peak. The upper level is not occupied and does not participate.

This mechanism can be generalized to many ( $N$ ) levels, where the role of the  $f_{1\sigma}$  level is played by the “sum” over or the superposition of all levels. One level after the other is shifted to higher energies, and only one broad ( $\sim N\Gamma$ ) level

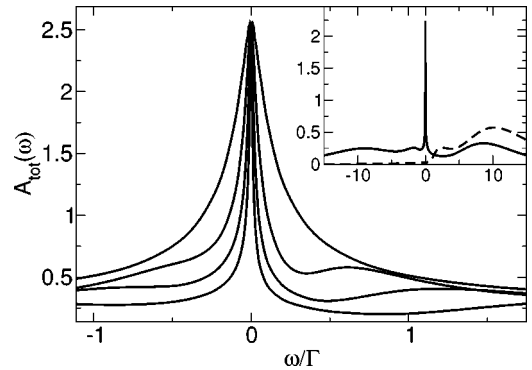


FIG. 5. Effective density of states for a multilevel Kondo dot with increasing level splitting. The lower level sits at  $2\pi\epsilon_1=-25$  and the upper level at  $2\pi\epsilon_2=-25, -23.75, -22.5, \text{ and } -20$  (outermost to innermost curve, everything in units of  $\Gamma$ ). The inset shows the spectral densities of the lower (solid line) and upper level (dashed line) for  $2\pi\epsilon_2=-20$ . Common parameters are  $2\pi U=50$ ,  $2\pi D=25$ ,  $\phi=0$ ,  $T=0$ .

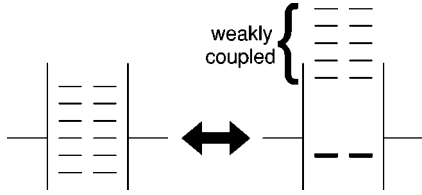


FIG. 6. Scheme of the effect of the renormalization group for a multilevel quantum dot. One broadened level remains while the others are moved to higher energies and weaker coupling.

remains, as sketched in Fig. 5. This new, broad level alone participates in the Kondo effect, which shows a strongly increased  $T_K$ , making it much easier to observe. We suggest that this mechanism explains the observed single-level Kondo physics in QDs, in the sense that although multilevel physics should be expected, the single-level Kondo effect is a good description and prevails, the difference being what the single level is made of.

We conclude that even for many spin-degenerate levels (with nonconserved orbital index) only a single Kondo peak is seen. The Kondo temperature depends on the level splittings. The other excitations can be traced back to shoulders as discussed in Refs. 23, 24, and 29. In two parallel QDs the level splitting is easily tunable, which allows to directly measure the change of  $T_K$ .

## V. PARALLEL QUANTUM DOTS

In this section we study the physics of two parallel, interacting quantum dots as previously introduced, which can be tuned by an AB phase. First we focus on the special case  $\phi = \pi$ , which corresponds to a Kondo-like situation, then we investigate the behavior when moving away from the special point. Note that this does not necessarily require parallel QDs but can also be realized in multilevel dots, when for instance one level is symmetric and the other antisymmetric.

### A. Interference-induced orbital Kondo effect

As mentioned before, the case  $\phi = \pi$  plus  $T_1 = T_2$  corresponds to a model where one level couples only to the left and the other one only to the right, as shown in Fig. 6. Evidently there are two conserved quantities: the spin and a geometrical pseudospin (left/right). Introducing symmetric and antisymmetric combinations of the lead states  $b_{ki\sigma} = a_{kR\sigma} - (-1)^i a_{kL\sigma}$ , we can rewrite the tunneling part of the Hamiltonian as

$$H_T = \sum_{ki\sigma} T_i b_{ki\sigma}^\dagger c_{i\sigma} + \text{H.c.} \quad (6)$$

This has the form of an Anderson Hamiltonian with the two conserved quantities discussed before. One therefore finds an enhanced Kondo effect for a low lying level at low temperatures. In other words, the state of complete destructive interference is a strong coupling state. Such models have been studied, for instance, for multilevel vertical quantum dots,<sup>37</sup> where the orbital momentum is conserved in tunneling, or in double-layer QD system,<sup>18-21</sup> where the index  $i$  corresponds

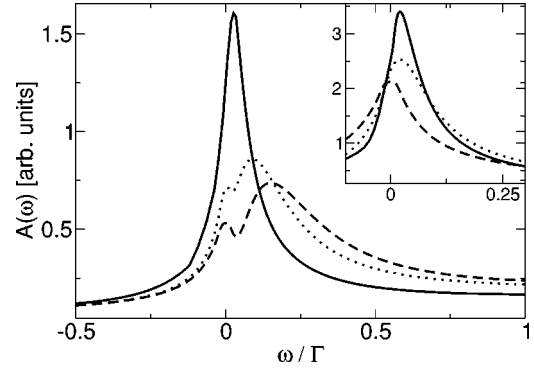


FIG. 7. Spectral density  $A(\omega)$  of level 1 (main panel) and effective density of states (inset). The phase  $\phi$  is changed from 0 (dashed line), over  $\pi/2$  (dotted line) to the value of the interference-induced orbital Kondo effect,  $\phi = \pi$  (solid line). Parameters for the symmetric dots are in units of  $\Gamma$ :  $U = 50/2\pi$ ,  $\epsilon_1 = \epsilon_2 = -25/2\pi$ ,  $D = 25/2\pi$ ,  $T = 0$ .

to the upper or lower plane. In such cases the Kondo temperature is enhanced with respect to a pure spin Kondo model, as the second quantum number—the pseudospin—can give rise to Kondo correlations alone. This is true also in our case, where strong correlations can be expected even without spin. In Fig. 7 we show the spectral density corresponding to  $c_{1\sigma}$ . For zero phase a weak Kondo peak and a second broader peak at higher frequencies are visible. The broad peak (essentially the shoulder discussed before) moves to lower frequencies when the phase is increased towards  $\pi$  and merges with the Kondo resonance for  $\phi = \pi$ . This strengthens the peak and thus enhances the Kondo temperature  $T_K$  as can be seen more clearly in the inset, where the density of states of the  $f_{1\sigma}$  level is shown. Note that one of the special features of this Kondo effect is that the tunneling matrix elements are tunable for each (pseudo) spin, as the individual levels can be controlled.

We remark that the Kondo effect discussed here is qualitatively different from an orbital Kondo effect as discussed in Ref. 19 and also from two-channel Kondo physics.<sup>38-41</sup>

### B. Splitting the Kondo peak

The ordinary Kondo effect in quantum dots can be destroyed by the application of either a magnetic field that splits the level by the Zeeman energy  $\Delta_Z$  or by a bias voltage introducing dephasing<sup>42-44</sup> (where the latter might under certain conditions open the door for two-channel Kondo physics again<sup>44,45</sup>). In our case the orbital Kondo effect can be destroyed by the analog of the Zeeman term which is the level splitting, by different tunneling amplitudes (not accessible in ordinary QDs), by a bias voltage in the usual sense, and via a detuning of the phase, i.e., away from  $\phi = \pi$ .

An interesting question is whether a splitting of the levels leads to a splitting of the Kondo peak, the development of satellite peaks, or is only a weakening and destruction of the Kondo peak is observed. In Fig. 8 we find that a peak splitting can only be observed if both, the Zeeman and the orbital level splitting, are introduced. No side peaks appear if only one of them is present, which only leads to a reduction of

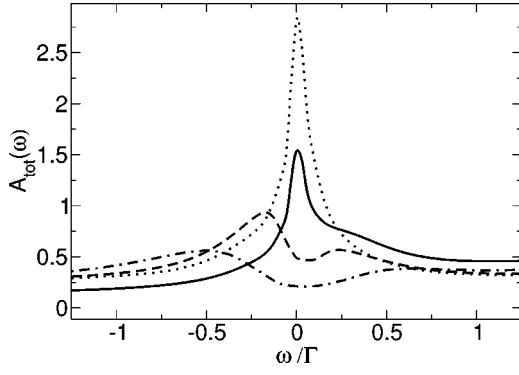


FIG. 8. Effective density of states at  $\phi = \pi$  under the influence of Zeeman and level splitting. No peak splitting can be seen for the combination  $\Delta_Z = 0.25$  and  $\epsilon_2 = -2.5$  (dotted line) or for  $\Delta_Z = 0$  and  $\epsilon_2 = -2.75$  (solid line). If both splittings are introduced at the same time a peak splitting is seen for  $\Delta_Z = 0.25$  and  $\epsilon_2 = -2.75$  (dashed line) and  $\Delta_Z = 0.5$  and  $\epsilon_2 = -3$  (dot-dashed line). Parameters for the symmetric dots are in units of  $\Gamma$ :  $U = 5$ ,  $\epsilon_1 = \epsilon_2 = -2.5$ ,  $D = 2.5$ ,  $T = 0$ .

$T_K$ . The suppression of side peaks has been attributed to an enhanced dephasing rate, such as produced by spinflip cotunneling.<sup>42,43,46</sup>

Note that this result also applies to other geometries such as double-layer QDs.<sup>18–21</sup>

### C. Detection

The detection of an interference-induced orbital Kondo effect is more difficult than for the usual spin Kondo effect. Nevertheless, it is possible by probing the resonance by additional leads to the dot.<sup>47–49</sup> If the coupling is weak enough one can perform spectroscopic measurements on the spectral densities in the individual dots. Another method is to measure the transport and noise properties of a quantum point contact which is in the vicinity<sup>50</sup> of the double dot system. In contrast to the spin Kondo effect, the up and down pseudospins correspond to charges in the upper or lower dot, which are much easier to detect. The strong fluctuations in the Kondo regime will therefore influence the transmission properties of the point contact allowing an indirect measurement of the Kondo resonance, in a way which is not accessible for the usual spin Kondo effect. The measurement of charge fluctuations thus provides a direct handle on spin fluctuations.

In real QD systems complete destructive interference, where the dots become opaque, is not achieved experimentally. The reasons are the difficulty to realize exactly equal QDs, as well as effects not captured in our model, such as more levels (at higher energy) or processes that break the phase coherence of an otherwise coherent process (less relevant at low temperatures). Yet, more than 50% contrast is possible in today's experiments<sup>5</sup> and the effect is therefore observable.

## VI. CONCLUSIONS

We studied coherence in two interacting quantum dot systems. First we investigated multilevel QDs with spin. We

discussed the relevant excitations and energy scales. The multilevel Kondo effect has been analyzed. We demonstrated that single-level Kondo physics essentially prevails, and that the corresponding Kondo temperature can be strongly enhanced. We have also investigated a very similar system, namely, two single-level (but spin degenerate) QDs in parallel. Their behavior can be tuned by an enclosed magnetic flux. We showed that coherence persists when the two dots interact with each other. In the case of destructive interference, the system exhibits a different Kondo behavior (interference-induced orbital Kondo effect) that is not due to the spin degree of freedom and allows to access Kondo correlations via charge fluctuations. Side peaks in the density of states appear only if a Zeeman and a level splitting are introduced together.

## ACKNOWLEDGMENTS

We would like to thank S. Kleff, J. König, J. Kroha, T. Pohjola, A. Rosch, G. Schön, and D. Vollhardt for useful discussions. This work was supported by the DFG through Graduiertenkolleg ‘‘Kollektive Phänomene im Festkörper’’ and the CFN (D.B.), as well as through SFB 484 and a postdoctoral research grant (W.H.).

## APPENDIX: SCHRIEFFER-WOLFF TRANSFORMATION

We perform a unitary transformation on the Hamiltonian Eq. (1) such that the unoccupied and doubly occupied states are projected out

$$H' = e^S H e^{-S} = H_0 + \frac{1}{2} [S, H_T] + \dots, \quad (\text{A1})$$

where  $S$  has been chosen to fulfill  $[S, H_0] = -H_T$ . In our case this operator is given by

$$S = \sum_{krs\sigma} T_{ks\sigma}^{r,*} \left( \frac{1 - (n_{s\sigma}^- + n_{s\sigma}^- + n_{s\sigma}^-)}{\epsilon_{s\sigma} - \epsilon_{kr}} + \frac{n_{s\sigma}^- + n_{s\sigma}^- + n_{s\sigma}^-}{\epsilon_{s\sigma} + U - \epsilon_{kr}} \right) c_{s\sigma}^\dagger a_{kr\sigma} - \text{H.c.} \quad (\text{A2})$$

To avoid cluttering the notation we suppress the indices on the tunneling matrix elements and local energies from now on, and take  $U \rightarrow \infty$ . We introduce two new coupling constants,

$$J_k = - \frac{|T|^2}{\epsilon - \epsilon_k}, \quad (\text{A3})$$

$$\Delta_0 = \sum_{kr} J_k, \quad (\text{A4})$$

The new Hamiltonian is finally given by

$$H = H_0 + \left[ -\Delta_0 \sum_{ss'\sigma} c_{s\sigma}^\dagger c_{s'\sigma} + \sum_{krk'r'\sigma} J_k n_{s\sigma} a_{k'r'\sigma}^\dagger a_{kr\sigma} + \sum_{krk'r'\sigma} J_k (c_{s\sigma}^\dagger c_{s\sigma}^- a_{k'r'\sigma}^\dagger a_{kr\sigma} + c_{s\sigma}^\dagger c_{s\sigma}^- a_{k'r'\sigma}^\dagger a_{kr\sigma} + c_{s\sigma}^\dagger c_{s\sigma}^- a_{k'r'\sigma}^\dagger a_{kr\sigma} + c_{s\sigma}^\dagger c_{s\sigma}^- a_{k'r'\sigma}^\dagger a_{kr\sigma}) \right]. \quad (\text{A5})$$

Replacing the dot operators by the (anti) symmetric combinations  $f_{1/2\sigma}$ , we obtain

$$H = H_0^{\text{res}} + \frac{\epsilon_1 + \epsilon_2}{2} (f_{1\sigma}^\dagger f_{1\sigma} + f_{2\sigma}^\dagger f_{2\sigma}) + \sum_{\sigma} \delta \epsilon (f_{1\sigma}^\dagger f_{2\sigma} + \text{H.c.}) - \Delta_0 \sum_{\sigma} f_{1\sigma}^\dagger f_{1\sigma} + \sum_{krk'r'\sigma} J_k (a_{kr\sigma}^\dagger a_{k'r'\sigma} f_{1\sigma}^\dagger f_{1\sigma} + a_{kr\sigma}^\dagger a_{k'r'\sigma} f_{1\sigma}^\dagger f_{1\sigma}). \quad (\text{A6})$$

\*Electronic address: dboese@tfp.physik.uni-karlsruhe.de

<sup>†</sup>Present address: Lyman Laboratory, Harvard University, Cambridge, MA 02138.

<sup>1</sup>A. Yacoby, M. Heiblum, H. Shtrikman, and D. Mahalu, *Phys. Rev. Lett.* **74**, 4047 (1995).

<sup>2</sup>R. Schuster *et al.*, *Nature (London)* **385**, 417 (1997).

<sup>3</sup>W.G. van der Wiel *et al.*, *Science* **289**, 2105 (2000).

<sup>4</sup>Y. Ji, M. Heiblum, D. Sprinzak, D. Mahalu, and H. Shtrikman, *Science* **290**, 779 (2000).

<sup>5</sup>A.W. Holleitner, C.R. Dekker, H. Qin, K. Eberl, and R.H. Blick, *Phys. Rev. Lett.* **87**, 256802 (2001).

<sup>6</sup>A.L. Yeyati and M. Büttiker, *Phys. Rev. B* **52**, 14 360 (1995).

<sup>7</sup>C. Bruder, R. Fazio, and H. Schoeller, *Phys. Rev. Lett.* **76**, 114 (1996).

<sup>8</sup>Y. Oreg and Y. Gefen, *Phys. Rev. B* **55**, 13 726 (1997).

<sup>9</sup>D. Loss and E.V. Sukhorukov, *Phys. Rev. Lett.* **84**, 1035 (2000).

<sup>10</sup>E. Buks, R. Schuster, M. Heiblum, D. Mahalu, and V. Umansky, *Nature (London)* **391**, 871 (1998).

<sup>11</sup>S. Kirchner, J. Kroha, and E. Scheer, in *Proceedings of the NATO Advanced Research Workshop "Size Dependent Magnetic Scattering," Pecs, Hungary, 2000*, edited by V. Chandrasekhar, C.V. Haesendonck, and A. Zawadowski (Kluwer Academic, Dordrecht, 2001) S. Kirchner, J. Kroha, and E. Scheer, cond-mat/0010103 (unpublished).

<sup>12</sup>F. Reinert *et al.*, *Phys. Rev. Lett.* **87**, 106401 (2001).

<sup>13</sup>J. Goeres *et al.*, *Phys. Rev. B* **62**, 2188 (2000).

<sup>14</sup>W. Hofstetter, J. König, and H. Schoeller, *Phys. Rev. Lett.* **87**, 156803 (2001).

<sup>15</sup>B.R. Bulka and P. Stefanski, *Phys. Rev. Lett.* **86**, 5128 (2001).

<sup>16</sup>L.I. Glazman and R.E. Raikh, *Pis'ma Zh. Éksp. Teor. Fiz.* **47**, 378 (1988) [*JETP Lett.* **47**, 452 (1988)].

<sup>17</sup>T.K. Ng and P.A. Lee, *Phys. Rev. Lett.* **61**, 1768 (1988).

<sup>18</sup>T. Pohjola, D. Boese, J. König, H. Schoeller, and G. Schön, *J. Low Temp. Phys.* **118**, 391 (2000).

<sup>19</sup>T. Pohjola, H. Schoeller, and G. Schön, *Europhys. Lett.* **54**, 241 (2001).

<sup>20</sup>U. Wilhelm and J. Weis, *Physica B* **6**, 668 (2000).

<sup>21</sup>U. Wilhelm, J. Schmid, J. Weis, and K.v. Klitzing, *Physica B* **9**, 625 (2001).

<sup>22</sup>J. König and Y. Gefen, *Phys. Rev. Lett.* **86**, 3855 (2001).

<sup>23</sup>D. Boese, W. Hofstetter, and H. Schoeller, *Phys. Rev. B* **64**, 125309 (2001).

<sup>24</sup>D. Boese, *Quantum Transport Through Nanostructures: Quantum Dots, Molecules and Quantum Wires* (Shaker Verlag, Aachen, 2002).

<sup>25</sup>K.G. Wilson, *Rev. Mod. Phys.* **47**, 773 (1975).

<sup>26</sup>T.A. Costi, A.C. Hewson, and V. Zlatić, *J. Phys.: Condens. Matter* **6**, 2519 (1994).

<sup>27</sup>W. Hofstetter, *Phys. Rev. Lett.* **85**, 1508 (2000).

<sup>28</sup>W. Hofstetter and H. Schoeller, *Phys. Rev. Lett.* **88**, 016803 (2002).

<sup>29</sup>T. Inoshita *et al.*, *Phys. Rev. B* **48**, 14 725 (1993).

<sup>30</sup>J. König, Y. Gefen, and G. Schön, *Phys. Rev. Lett.* **81**, 4468 (1998).

<sup>31</sup>J. König and Y. Gefen, *Phys. Rev. B* **65**, 045316 (2002).

<sup>32</sup>P.G. Silvestrov and Y. Imry, *Phys. Rev. Lett.* **85**, 2565 (2000).

<sup>33</sup>P.G. Silvestrov and Y. Imry, cond-mat/0102088 (unpublished).

<sup>34</sup>W. Izumida, O. Sakai, and Y. Shimizu, *J. Phys. Soc. Jpn.* **66**, 717 (1997).

<sup>35</sup>W. Izumida, O. Sakai, and Y. Shimizu, *J. Phys. Soc. Jpn.* **67**, 2444 (1998).

<sup>36</sup>A.L. Chudnovskiy and S.E. Ulloa, *Phys. Rev. B* **63**, 165316 (2001).

<sup>37</sup>T. Pohjola *et al.*, *Europhys. Lett.* **40**, 189 (1997).

<sup>38</sup>K.A. Matveev, *Zh. Éksp. Teor. Fiz.* **99**, 1598 (1991) [*Sov. Phys. JETP* **72**, 892 (1991)].

<sup>39</sup>K. Vladar and A. Zawadowski, *Phys. Rev. B* **28**, 1564 (1983).

<sup>40</sup>A. Zawadowski, J.v. Delft, and D.C. Ralph, *Phys. Rev. Lett.* **83**, 2632 (1999).

<sup>41</sup>D.L. Cox and A. Zawadowski, *Adv. Phys.* **47**, 599 (1998).

<sup>42</sup>A. Kaminski, Y.V. Nazarov, and L.I. Glazman, *Phys. Rev. Lett.* **83**, 384 (1999).

<sup>43</sup>A. Kaminski, Y.V. Nazarov, and L.I. Glazman, *Phys. Rev. B* **62**, 8154 (2000).

<sup>44</sup>A. Rosch, J. Kroha, and P. Wölfle, *Phys. Rev. Lett.* **87**, 156802 (2001).

<sup>45</sup>P. Coleman, C. Hooley, and O. Parcolle, *Phys. Rev. Lett.* **86**, 4088 (2001).

<sup>46</sup>Y. Meir, N.S. Wingreen, and P.A. Lee, *Phys. Rev. Lett.* **70**, 2601 (1993).

<sup>47</sup>Q. Sun and H. Guo, *Phys. Rev. B* **64**, 153306 (2001).

<sup>48</sup>E. Lebanon and A. Schiller, cond-mat/0105488 (unpublished).

<sup>49</sup>S. di Francesco (private communication).

<sup>50</sup>D. Sprinzak, Y. Ji, M. Heiblum, D. Mahalu, and H. Shtrikman, cond-mat/0109402.